Vol 18 No 2, February 2009
1674-1056/2009/18(02)/0749-08

Chinese Physics B

© 2009 Chin. Phys. Soc.
and IOP Publishing Ltd

The influence of the Dresselhaus spin–orbit coupling on the tunnelling magnetoresistance in ferromagnet/ insulator /semiconductor/ insulator /ferromagnet tunnel junctions*

Wang Xiao-Hua(王晓华)[a], An Xing-Tao(安兴涛)[a], and Liu Jian-Jun(刘建军)[a)b)†]

[a)] *College of Physical Science and Information Engineering, Hebei Normal University, Shijiazhuang* 050016, *China*

[b)] *Hebei Advanced Thin Films Laboratory, Shijiazhuang* 050016, *China*

(Received 13 October 2008; revised manuscript received 21 October 2008)

This paper investigates the effect of Dresselhaus spin–orbit coupling on the spin-transport properties of ferromagnet/insulator/semiconductor/insulator/ferromagnet double-barrier structures. The influence of the thickness of the insulator between the ferromagnet and the semiconductor on the polarization is also considered. The obtained results indicate that (i) the polarization can be enhanced by reducing the insulator layers at zero temperature, and (ii) the tunnelling magnetoresistance inversion can be illustrated by the influence of the Dresselhaus spin–orbit coupling effect in the double-barrier structure. Due to the Dresselhaus spin–orbit coupling effect, the tunnelling magnetoresistance inversion occurs when the energy of a localized state in the barrier matches the Fermi energy $E_{\rm F}$ of the ferromagnetic electrodes.

Keywords: Dresselhaus spin–orbit coupling, ferromagnet/insulator/semiconductor/insulator/ferromagnet double-barrier structures, transfer-matrix method

PACC: 7210, 7335, 7290

1. Introduction

Recently, spin-polarized transport[1−3] has attracted a rapidly growing attention due to its potential applications to spin-electronic devices. One of the main challenges of spintronics today is to combine ferromagnet (FM) and semiconductor (SM) properties.[4,5] Due to its fundamental importance and potential microelectronic applications, a typical FM/SM/FM[6] nanostructure where electronic spin injection from FM into SM has attracted intensive research interest, both experimentally and theoretically.[5,7−13] The most well-known spintronics device is the spin transistor based on spin precession controlled by an external electrical field via spin–orbit coupling (SOC) proposed by Datta and Das,[7] but this has yet to be realized experimentally.

The tunnelling magnetoresistance (TMR) is another important character which was observed by Julliere[14] in a tunnel junction consisting of two thick ferromagnetic layers and a thin insulator layer (IN). The TMR is widely used in readout devices and nonvolatile memory cells.[5,15,16] Recently, some experimental groups discussed different mechanisms for the inverse TMR effect through different magnetic tunnel junctions.[17−22] Tsymbal *et al*[17] observed that resonant tunnelling via localized states in the barrier can invert magnetoresistance in magnetic tunnel junctions. Teresa *et al*[18] proposed that different polarity of the spin polarization of two contacts can lead to the TMR inversion. Mukhopadhyay *et al*[20] believe that the TMR undergoes a change of sign at higher bias and temperature. This phenomenon is attributed to the competition between the spin conserved ballistic transport through the pinhole contact where the transmission probability is close to unity and spin polarized tunnelling is across the insulating spacer with weak transmittivity. Chantis *et al*[21] demonstrated that the observed reversal of the spin polarization in Fe/GaAs(001) tunnel contacts is intrinsic to their in-

*Project supported by the National Natural Science Foundation of China (Grant No 10674040) and the Specialized Research Fund for the Doctoral Program of Higher Education of China (Grant No 20060094002).

†Corresponding author. E-mail: liujj@mail.hebtu.edu.cn

terface electronic structure. This explains the experimental findings of anomalous bias dependence of the spin polarization in experiments on TMR. Moser *et al*[22] found that TMR changes sign with bias voltage at the epitaxial Fe/GaAs(001) interface. Different mechanisms mentioned above about the TMR inversion indicate that the reason of the TMR inversion is different for various structures.

This paper studies the spin polarization and the TMR inversion for the ferromagnet/insulator/semiconductor/insulator/ferromagnet (FM/IN/SM/IN/FM) double junction. Due to the thin oxide layers at the interfaces between the FM and the SM caused by the experimental preparation technique, the thickness of the INs between the FM and the SM should be considered theoretically. The effects of the Dresselhaus SOC on spin polarization and TMR are investigated. Using the Airy function, we study spin-dependent transport through FM/IN/SM/IN/FM double tunnel junctions subjected to an electric field.[23] We consider the difference of electron effective masses in three different material regions and the intrinsic conductivity mismatch between ferromagnetic metal and semiconductors.[24] Our treatment still relies on the free-electron model of the conduction electrons to study the spin-polarized transport properties through the FM/SM/FM junctions. This model is relatively simple and has been adopted with success to study the spin-polarized tunnelling between iron-group ferromagnetic metals and the tunnelling through FM/SM(IN)/FM junctions.

2. Model and method

We divide the double tunnel junction into five regions (1, 2, 3, 4, and 5). The state densities of spin-up (+) and spin-down (−) electrons in the ferromagnetic substance and the schematic potential are shown in Fig.1.

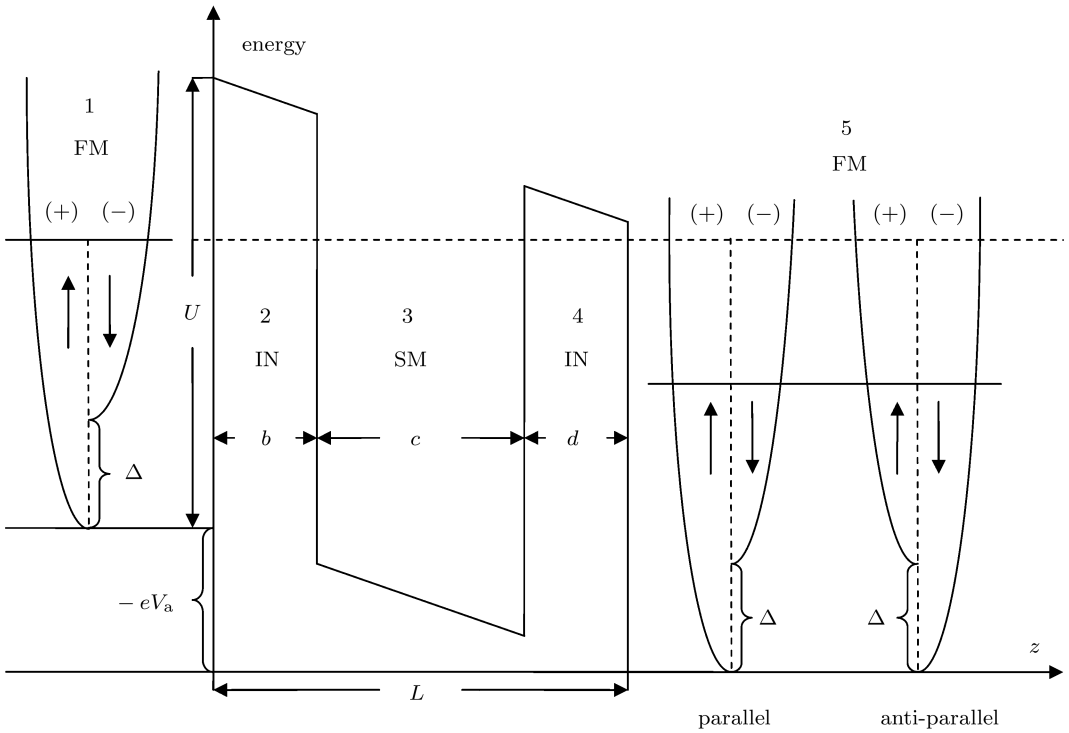


Fig.1. The state densities of spin-up (+) and spin-down (−) electrons in the ferromagnetic substance and the schematic potential for the FM/IN/SM/IN/FM structure in an applied positive bias V_a. In the ferromagnetic substance, the band of electrons with minority spins (−) is shifted by Δ with respect to the majority band (+). L is the width of the double-barrier structure. c is the width of the middle SM. b and d are the width of the left and right barriers, respectively. U is the barrier height.

Based on the simple free-electron approximation of the spin-polarized conduction electrons, we can write the effective one-electron Hamiltonian as (in the FM and IN regions)

$$H = -\frac{\hbar^2}{2m_j^*}\nabla^2 - F(z) + U(z) - \boldsymbol{h}(z)\cdot\boldsymbol{\sigma} \quad (j = 1, 2, 4 \text{ and } 5) \tag{1}$$

for the positive bias. Where

$$F(z) = \begin{cases} 0, & z < 0, \\ eV_{\mathrm{a}}z/L, & 0 < z < L, \\ eV_{\mathrm{a}}, & z > L, \end{cases} \tag{2}$$

and m_j^*, $j = 1, 2, 4$, and 5, stands for the electron effective masses in the different material regions. The $\boldsymbol{h}(z)\cdot\boldsymbol{\sigma}$ represents the internal exchange energy, here $\boldsymbol{h}(z)$ is the molecular field and $\boldsymbol{\sigma}$ is the conventional Pauli spin operator. It is assumed in this model that $\boldsymbol{h} = 0$ within the IN and SM layers, and $|\boldsymbol{h}| = h_0$ within each FM layer, where h_0 is equal to $\dfrac{\Delta}{2}$. Δ is the exchange splitting energy in the ferromagnetic substance. $U(z) = 0$ for the two FM layers and the SM layer, and $U(z) = U$ for the two INs.

In the SM region, we consider the transmission of electrons with the initial wave vector $\boldsymbol{k} = (\boldsymbol{k}_{\parallel},\ k_z)$ through the double barrier structure grown along the z direction. Here, $\boldsymbol{k}_{\parallel}$ is wave vector in the plane of the interfaces and k_z is a component of wave vector in the direction of tunnelling. The electron motion in the SM region is described by the Hamiltonian

$$H_{\mathrm{s}} = -\frac{\hbar^2}{2m_3^*}\nabla^2 - F(z) + \delta E_{\mathrm{c}} + H_{\mathrm{D}}, \tag{3}$$

where m_3^* is the electron effective mass in the SM region, δE_{c} is the conduction band mismatch between the FM and SM, H_{D} is the Hamiltonian of the Dresselhaus SOC term caused by the bulk inversion asymmetry and it exists broadly in the widely used III–V compound SMs with zinc-blende crystal structures.[25] The Hamiltonian of the Dresselhaus SOC can be written as[26] $H_{\mathrm{D}} = \gamma(\sigma_x k_x - \sigma_y k_y)\dfrac{\partial^2}{\partial z^2}$, where γ is the Dresselhaus parameter denoting the strength of the coupling, σ_x and σ_y are the Pauli matrices. The Dresselhaus SOC term can be diagonalized by the spinors $\chi_{\pm}$.[27] The effective Hamiltonian in the SM has the form

$$H_{\pm} = -\frac{\hbar^2}{2m_{\pm}}\frac{\partial^2}{\partial z^2} + \frac{\hbar^2 k_{\parallel}^2}{2m_3^*} - F(z) + \delta E_{\mathrm{c}}, \tag{4}$$

where

$$m_{\pm} = m_3^*\left(1 \pm 2\frac{\gamma m_3^* k_{\parallel}}{\hbar^2}\right)^{-1}. \tag{5}$$

Therefore, the Dresselhaus SOC effect on the spin-up and the spin-down electrons is equivalent to a spin-dependent modification of the effective mass.

In the FM regions, we use a plane-wave approximation. The wave functions of carriers with majority and minority spins in the left and right electrodes are

$$\psi_{1\sigma} = A_{1\sigma}\mathrm{e}^{\mathrm{i}k_{1\sigma}z} + B_{1\sigma}\mathrm{e}^{-\mathrm{i}k_{1\sigma}z} \quad (z < 0), \tag{6}$$

$$\psi_{5\sigma} = A_{5\sigma}\mathrm{e}^{\mathrm{i}k_{5\sigma}z} + B_{5\sigma}\mathrm{e}^{\mathrm{i}k_{5\sigma}z} \quad (z > b + c + d), \tag{7}$$

respectively. Where

$$k_{1\uparrow} = \sqrt{2m_1^* E_{\mathrm{f}}/\hbar^2 - k_{\parallel}^2},$$
$$k_{1\downarrow} = \sqrt{2m_1^*(E_{\mathrm{f}} - \Delta)/\hbar^2 - k_{\parallel}^2},$$
$$k_{5\uparrow} = \sqrt{2m_5^*(E_{\mathrm{f}} + eV_{\mathrm{a}})/\hbar^2 - k_{\parallel}^2}$$

and

$$k_{5\downarrow} = \sqrt{2m_5^*(E_{\mathrm{f}} + eV_{\mathrm{a}} - \Delta)/\hbar^2 - k_{\parallel}^2}$$

are the Fermi wave vectors of the majority and minority subbands, respectively, $\sigma = \pm 1$ corresponds to $\sigma = \uparrow, \downarrow$, respectively, E_{f} is the Fermi energy with respect to the bottom of the majority band.

In the SM and the IN regions, the Schrödinger equation can be written by a simple coordinate transformation whose solutions are the Airy function $\mathrm{Ai}[\rho(z)]$ and its complement $\mathrm{Bi}[\rho(z)]$. The general solution of the Schrödinger equation for the positive bias is given as

$$\psi_{j\sigma}(z) = \begin{cases} A_{2\sigma}\mathrm{Ai}[\rho_{2\sigma}(z)] + B_{2\sigma}\mathrm{Bi}[\rho_{2\sigma}(z)], & 0 < z < b \quad (j = 2) \\ A_{3\sigma}\mathrm{Ai}[\rho_{3\sigma}(z)] + B_{3\sigma}\mathrm{Bi}[\rho_{3\sigma}(z)], & b < z < b + c \quad (j = 3) \\ A_{4\sigma}\mathrm{Ai}[\rho_{4\sigma}(z)] + B_{4\sigma}\mathrm{Bi}[\rho_{4\sigma}(z)], & b + c < z < b + c + d \quad (j = 4) \end{cases} \tag{8}$$

where $\rho_{j,\sigma}(z) = \dfrac{z}{\lambda_{0j}} + \beta_{0j,\sigma}$, ($j = 2$, 3 and 4), here

$$\lambda_{0j} = \begin{cases} \left[-\dfrac{\hbar^2 L}{2m_2^* e V_\mathrm{a}}\right]^{-\frac{1}{3}} & (j=2), \\ \left[-\dfrac{\hbar^2 L}{2m_\pm^* e V_\mathrm{a}}\right]^{-\frac{1}{3}} & (j=3), \\ \left[-\dfrac{\hbar^2 L}{2m_4^* e V_\mathrm{a}}\right]^{-\frac{1}{3}} & (j=4), \end{cases}$$

and

$$\beta_{0j,\sigma} = \begin{cases} \dfrac{L\left(E_\mathrm{f} - U - \dfrac{\hbar^2 k_\parallel^2}{2m_2^*}\right)}{eV_\mathrm{a}\lambda_{02}} & (j=2), \\ \dfrac{L\left(E_\mathrm{f} - \delta E - \dfrac{\hbar^2 k_\parallel^2}{2m_3^*}\right)}{eV_\mathrm{a}\lambda_{03}} & (j=3), \\ \dfrac{L\left(E_\mathrm{f} - U - \dfrac{\hbar^2 k_\parallel^2}{2m_4^*}\right)}{eV_\mathrm{a}\lambda_{04}} & (j=4), \end{cases}$$

are the parameters, respectively.

According to the solution of the Schrödinger equation with the Hamiltonians (1) and (4) and the boundary conditions for the wave function at the interfaces, we can derive a matrix formula that connects the coefficients $A_{1\sigma}$ and $B_{1\sigma}$ with the coefficients $A_{5\sigma}$ and $B_{5\sigma}$ as $(A_{1\sigma}, B_{1\sigma})^\mathrm{T} = M_\mathrm{total}(A_{5\sigma}, B_{5\sigma})^\mathrm{T}$, where the total transfer matrix is

$$\begin{aligned} M_\mathrm{total} = {} & \begin{pmatrix} 1 & 1 \\ \dfrac{\mathrm{i}k_{1\sigma}}{m_1^*} & -\dfrac{\mathrm{i}k_{1\sigma}}{m_1^*} \end{pmatrix}^{-1} \begin{pmatrix} A_\mathrm{i}(\beta_{02}) & B_\mathrm{i}(\beta_{02}) \\ \dfrac{1}{m_2^*\lambda_{02}} A_\mathrm{i}'(\beta_{02}) & \dfrac{1}{m_2^*\lambda_{02}} B_\mathrm{i}'(\beta_{02}) \end{pmatrix} \\ & \begin{pmatrix} A_\mathrm{i}\left(\dfrac{b}{\lambda_{02}} + \beta_{02}\right) & B_\mathrm{i}\left(\dfrac{b}{\lambda_{02}} + \beta_{02}\right) \\ \dfrac{1}{m_2^*\lambda_{02}} A_\mathrm{i}'\left(\dfrac{b}{\lambda_{02}} + \beta_{02}\right) & \dfrac{1}{m_2^*\lambda_{02}} B_\mathrm{i}'\left(\dfrac{b}{\lambda_{02}} + \beta_{02}\right) \end{pmatrix}^{-1} \\ & \begin{pmatrix} A_\mathrm{i}\left(\dfrac{b}{\lambda_{03}} + \beta_{03}\right) & B_\mathrm{i}\left(\dfrac{b}{\lambda_{03}} + \beta_{03}\right) \\ \dfrac{1}{m_3^*\lambda_{03}} A_\mathrm{i}'\left(\dfrac{b}{\lambda_{03}} + \beta_{03}\right) & \dfrac{1}{m_3^*\lambda_{03}} B_\mathrm{i}'\left(\dfrac{b}{\lambda_{03}} + \beta_{03}\right) \end{pmatrix} \\ & \begin{pmatrix} A_\mathrm{i}\left(\dfrac{b+c}{\lambda_{03}} + \beta_{03}\right) & B_\mathrm{i}\left(\dfrac{b+c}{\lambda_{03}} + \beta_{03}\right) \\ \dfrac{1}{m_3^*\lambda_{03}} A_\mathrm{i}'\left(\dfrac{b+c}{\lambda_{03}} + \beta_{03}\right) & \dfrac{1}{m_3^*\lambda_{03}} B_\mathrm{i}'\left(\dfrac{b+c}{\lambda_{03}} + \beta_{03}\right) \end{pmatrix}^{-1} \\ & \begin{pmatrix} A_\mathrm{i}\left(\dfrac{b+c}{\lambda_{04}} + \beta_{04}\right) & B_\mathrm{i}\left(\dfrac{b+c}{\lambda_{04}} + \beta_{04}\right) \\ \dfrac{1}{m_4^*\lambda_{04}} A_\mathrm{i}'\left(\dfrac{b+c}{\lambda_{04}} + \beta_{04}\right) & \dfrac{1}{m_4^*\lambda_{04}} B_\mathrm{i}'\left(\dfrac{b+c}{\lambda_{04}} + \beta_{04}\right) \end{pmatrix} \\ & \begin{pmatrix} A_\mathrm{i}\left(\dfrac{b+c+d}{\lambda_{04}} + \beta_{04}\right) & B_\mathrm{i}\left(\dfrac{b+c+d}{\lambda_{04}} + \beta_{04}\right) \\ \dfrac{1}{m_4^*\lambda_{04}} A_\mathrm{i}'\left(\dfrac{b+c+d}{\lambda_{04}} + \beta_{04}\right) & \dfrac{1}{m_4^*\lambda_{04}} B_\mathrm{i}'\left(\dfrac{b+c+d}{\lambda_{04}} + \beta_{04}\right) \end{pmatrix}^{-1} \\ & \begin{pmatrix} \mathrm{e}^{\mathrm{i}k_{5\sigma}(b+c+d)} & \mathrm{e}^{-\mathrm{i}k_{5\sigma}(b+c+d)} \\ \dfrac{\mathrm{i}k_{5\sigma}}{m_5^*}\mathrm{e}^{\mathrm{i}k_{5\sigma}(b+c+d)} & -\dfrac{\mathrm{i}k_{5\sigma}}{m_5^*}\mathrm{e}^{-\mathrm{i}k_{5\sigma}(b+c+d)} \end{pmatrix}. \end{aligned}$$

Then, the transmission coefficient and the polarization for the double-barrier structure shown in Fig.1 are

$$T_{\sigma\sigma'} = \frac{k_{5\sigma}}{k_{1\sigma'}} \left| \frac{1}{M^{11}_{\text{total}}} \right|^2 , \tag{9}$$

and

$$P_{\uparrow\uparrow} = (T_{\uparrow\uparrow} - T_{\downarrow\downarrow})/(T_{\uparrow\uparrow} + T_{\downarrow\downarrow}), \tag{10}$$

respectively, where M^{11}_{total} is the left-upper element of the total transfer matrix. $P_{\uparrow\uparrow}$ is the polarization of the double tunnel junction with the magnetizations of the ferromagnetic electrodes aligned parallel to each other.

In the case of parallel magnetization of both FM layers, the total conductance is given by the transmission from the majority and minority bands into the corresponding majority and minority bands on the opposite side

$$G_{\uparrow\uparrow} = \frac{e^2}{h}(T_{\uparrow\uparrow} + T_{\downarrow\downarrow}). \tag{11}$$

For the antiparallel case the conductance is given by

$$G_{\uparrow\downarrow} = \frac{e^2}{h}(T_{\downarrow\uparrow} + T_{\uparrow\downarrow}). \tag{12}$$

The TMR can be expressed as

$$\text{TMR} = (G_{\uparrow\uparrow} - G_{\uparrow\downarrow})/G_{\uparrow\uparrow}. \tag{13}$$

3. Results and discussion

Taking the $Fe/Al_2O_3/GaAs/Al_2O_3/Fe$ double junction as an example, we assume $m_1 = m_5 = m_0$ in the Fe regions, $m_2 = m_4 = 0.23m_0$ in the INs (Al_2O_3),[28–31] and $m_3 = 0.067m_0$ in the SM (GaAs) region, where m_0 is the bare electron mass. The exchange splitting energy in the FMs is $\Delta = 3.46\,\text{eV}$ and the conduction band mismatch between the GaAs and the Fe $\delta E_c = 2.4\,\text{eV}$.[32] The Dresselhaus parameter $\gamma \approx 24\,\text{eV}\,\text{Å}^3$ (1 Å= 0.1 nm) in the GaAs region[27,33–36] and $\gamma = 0$ elsewhere. The GaAs is SM with relatively strong Dresselhaus SOC,[37] so other possible spin–orbit interactions such as the Rashba SOC contribution induced by the applied bias, have been neglected in this case. In this paper, the thickness of GaAs film (8 nm) is assumed to be shorter than the spin-flip length so that the spin-flip scattering can be neglected. At the same time, the thickness of GaAs film is long enough that the electrons tunnelling into the GaAs satisfy the Fermi distribution.

Figure 2 shows the polarization as a function of the positive bias when the INs have different thicknesses. The polarization increases as the thickness of the IN decreases at zero temperature. Compared with the results for the junctions with thick oxide layers, we find that the transmission probabilities for spin-up electrons are much higher than those for the spin-down electrons tunnelling through the junctions with thin oxide layers. In a recent experiment, Moser *et al*[22] investigated the polarization of Fe/GaAs junctions with different types of interfaces, oxidized interfaces and interfaces where the oxide is reduced by hydrogen plasma. They show that the polarization is enhanced by reducing the oxide layer using hydrogen plasma. Our calculated results qualitatively agree with those of Ref.[22] at zero temperature.

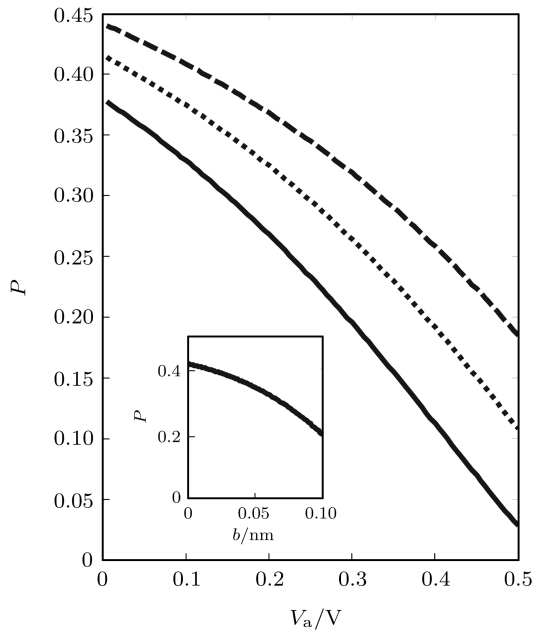


Fig.2. Bias dependence of the polarization for $Fe/Al_2O_3/GaAs(8\,\text{nm})/Al_2O_3/Fe$ junctions with $b = d = 0.1\,\text{nm}$ (solid curve), $b = d = 0.08\,\text{nm}$ (dotted curve), and $b = d = 0.06\,\text{nm}$ (dashed curve) for $k_{\parallel} = 2 \times 10^6\,\text{cm}^{-1}$. Other parameters are $U = 1.32\,\text{eV}$, temperature $T = 0$. The inset displays the polarization as a function of the thickness of the INs b and d.

To further explain the thickness of the IN effects on the polarization, the inset in Fig.2 shows the polarization as a function of the thickness of the IN. The polarization under a certain bias can be increased greatly by decreasing the thickness of the IN. We observe that the polarization increases from 0.2 to 0.41 when the thickness of the INs is reduced from 0.1 nm to near zero. Thus, the thickness of the INs should

be reduced experimentally in order to obtain higher polarization.

Figures 3(a) and 3(b) show the TMR as a function of the positive bias. In Fig.3(a) the Dresselhaus SOC in the SM is neglected. It shows that the TMR effect is positive with different in-plane wave vectors $k_{\|}$, i.e., the conductance for the parallel magnetization configuration is higher than that for the antiparallel alignment. In Fig.3(b) the TMR shows a positive value at $k_{\|} = 0$, while it has negative values as the $k_{\|}$ increases under a certain positive bias in the presence of the Dresselhaus SOC in the SM region.

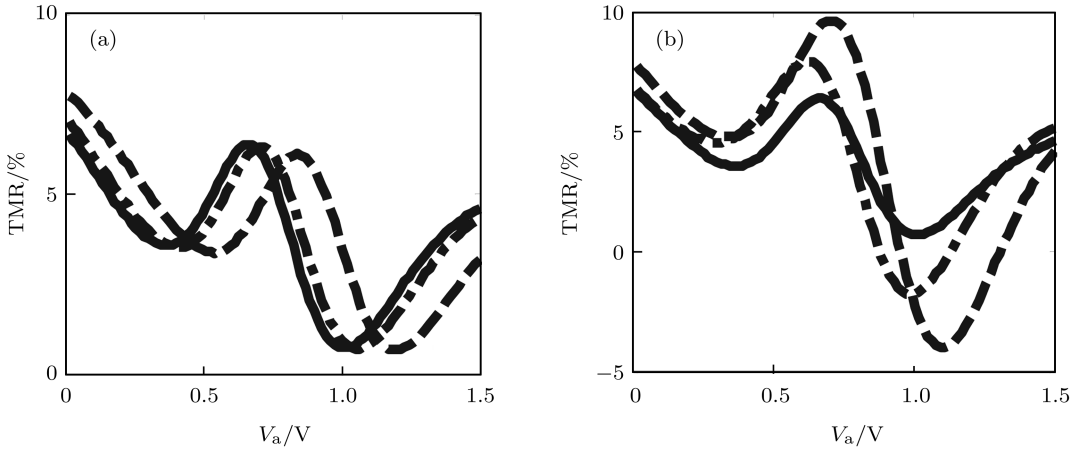


Fig.3. Bias dependence of the TMR for $Fe/Al_2O_3/GaAs(8\,nm)/Al_2O_3/Fe$ double tunnel junction with different in-plane wave vectors $k_{\|} = 0$ (solid curve), $k_{\|} = 2 \times 10^6\,cm^{-1}$ (dashdotted curve), $k_{\|} = 4 \times 10^6\,cm^{-1}$ (dashed curve). (a) The Dresselhaus parameter $\gamma = 0$. (b) The Dresselhaus parameter $\gamma \approx 24\,eV\text{Å}^3$.

Equation (5) indicates that the Dresselhaus SOC cannot affect the spin-transport properties of the tunnel junction when $k_{\|}$ is equal to zero. In SM region, the Dresselhaus SOC causes the resonant energy of spin-up and spin-down electrons to split at nonzero $k_{\|}$ because the Dresselhaus SOC lifts spin degeneracy. The influences of the Dresselhaus SOC on polarization and TMR should be considered. We demonstrate that the inversion of TMR might be caused by the Dresselhaus SOC.

In n-type zinc-blende semiconductors, a local magnetic field caused by SOC gives origin to a Zeeman-like splitting which, combined with the scattering, can cause a spin relaxation/dephasing known as the D'yakonov–Perel (DP) mechanism. The DP mechanism introduces a spin–orbit term in the Hamiltonian which can be expressed by a Zeeman-like term with a wave-vector-dependent effective magnetic field $H = \Omega(k)\cdot\sigma$. The effective g factor and the Bohr magneton are absorbed into the definition of $\Omega(k)$.[27] The GaAs which has the zinc blende structure is known to be semiconductor with relatively strong Dresslhaus SOC due to bulk inversion asymmetry. The Dresselhaus term is dominant in the DP wave-vector-dependent magnetic field, giving rise to a spin splitting. An external magnetic field can make the inversion of TMR, which has already been observed experimentally.[18,22] Similarly, the Dresselhaus SOC which acts as an effective magnetic field may also inverse the TMR.

Moreover, as the wave vectors $k_{\|}$ increase, the extremum of the TMR increases for the positive TMR and the negative TMR of the double tunnel junction.

Figures 4(a) and 4(b) show the transmission and TMR as a function of the positive bias, respectively. The transmission coefficient and the TMR, whether $k_{\|}$ is equal to zero or $5\times10^6\,cm^{-1}$, show obvious resonant features when electrons tunnel through the junctions.

A mechanism for inversion of the TMR was discussed previously: resonant tunnelling via localized states, i.e., the TMR is inverted when the energy of a localized state in the barrier matches the Fermi energy of the ferromagnetic electrodes.[17] Our results indicate that the inversion of the TMR cannot occur when $\gamma = 0$ or $k_{\|} = 0$ (see Figs.3(a) and 4(b)) although the transmission coefficient and the TMR show resonant features. The Dresselhaus SOC and the $k_{\|}$ are crucial to the observation of the TMR inversion. A positive TMR effect is observed at $k_{\|} = 0$ (solid curve in Fig.4(b)) and the inversion of the TMR can

occur at nonzero $k_{\|}$ (dashed curve in Fig.4(b)).

Although TMR inversion is not caused by resonant tunnelling in the FM/IN/SM/IN/FM double junction structure, the position of the TMR inversion is at the resonant peak via tuning the wave vector $k_{\|}$, i.e., the TMR inversion occurs when the energy of a localized state lies close to the E_{F} and resonant tunnelling dominates direct tunnelling. This inversion is believed to be due to the Dresselhaus SOC. Without the Dresselhaus SOC, the TMR inversion unlikely emerges even at the resonant tunnelling via localized states. The results may be useful for understanding and designing quantum spintronic devices.

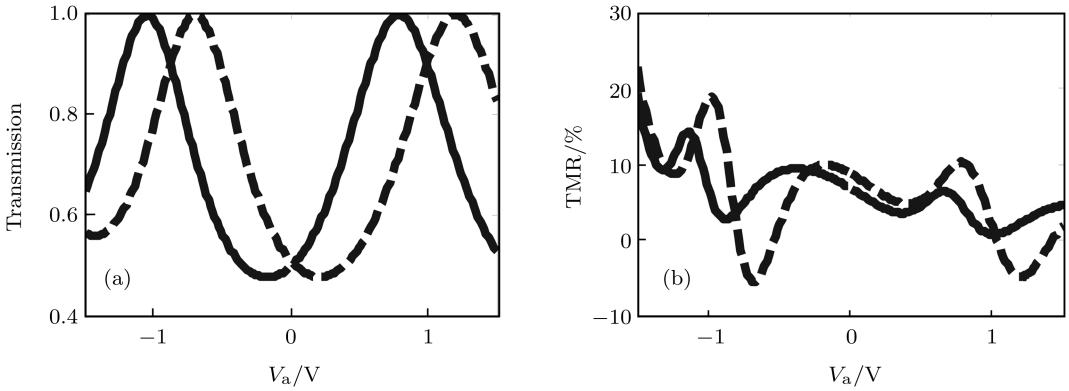


Fig.4. (a) Bias dependence of the transmission with $k_{\|} = 0$ (solid curve) and $k_{\|} = 5 \times 10^6\,\mathrm{cm}^{-1}$ (dashed curve), respectively. (b) Bias dependence of the TMR with $k_{\|} = 0$ (solid curve) and $k_{\|} = 5 \times 10^6\,\mathrm{cm}^{-1}$ (dashed curve), respectively.

4. Conclusion

In summary, using a transfer-matrix method, we investigate the transmission, polarization, and TMR of the FM/IN/SM/IN/FM double tunnel junction in the presence of the Dresselhaus SOC interaction and an electric field. It shows that the polarization is enhanced by decreasing the thickness of the INs. Our results indicate that the inversion of the TMR can emerge via a change of the in-plane $k_{\|}$ in the presence of Dresselhaus SOC. The results also indicate that the position of the TMR inversion corresponds to the resonance tunnelling via localized states. We hope that our results can stimulate interest in experimental efforts for designing spin-polarized resonant tunnelling devices.

References

[1] Gao Y F, Zhang Y P and Liang J Q 2005 *Chin. Phys.* **14** 196
[2] Li Z J 2005 *Chin. Phys.* **14** 2100
[3] Wang J M, Wang R and Liang J Q 2007 *Chin. Phys.* **16** 2075
[4] Prinz G A 1998 *Science* **282** 1660
[5] Wolf S A, Awschalom D D, Buhrman R A, Daughton J M, von Molnàr S, Roukes M L, Chtchelkanova A Y and Treger D M 2001 *Science* **294** 1488
[6] Li Y X and Li B Z 2005 *Chin.Phys.* **14** 1021
[7] Datta S and Das B 1990 *Appl. Phys. Lett.* **56** 665
[8] Bychkov Y A and Rashba E I 1984 *J. Phys.* C **17** 6039
[9] Luo J, Munekata H, Fang F F and Stiles P J 1990 *Phys. Rev.* B **41** 7685
[10] Nitta J, Akazaki T, Takayanagi H and Enoki T 1997 *Phys. Rev. Lett.* **78** 1335
[11] Hammar P R, Bennett B R, Yang M J and Johnson M 1999 *Phys. Rev. Lett.* **83** 203
[12] Alvorado S F 1995 *Phys. Rev. Lett.* **75** 513
[13] Guo Y, Chen X Y, Zhai F, Gu B L and Kawazoe Y 2002 *Appl. Phys. Lett.* **80** 4591
Zhai F, Guo Y and Gu B L 2003 *J. Appl. Phys.* **94** 5432
[14] Julliere M 1975 *Phys. Lett.* **54A** 225
[15] AwschalomD D, Loss D and Samarth N 2002 *Semiconductor Spintronics and Quantum Computation* (Berlin: Springer) p37
[16] Baibich M N, Broto J M, Fert A, Nguyen Van Dau F, Petroff F, Etienne P, Creuzet G, Friederich A and Chazelas J 1988 *Phys. Rev. Lett.* **61** 2472
[17] Tsymbal E Y, Sokolov A, Sabirianov I F and Doudin B 2003 *Phys. Rev. Lett.* **90** 186602
[18] De Teresa J M, Barthélémy A, Fert A, Contour J P, Lyonnet R, Montaigne F, Seneor P and Vaurès A 1999 *Phys. Rev. Lett.* **82** 4288

[19] Sharma M, Wang S X and Nickel J H 1999 *Phys. Rev. Lett.* **82** 616
[20] Mukhopadhyay S and Das I 2006 *Phys. Rev. Lett.* **96** 026601
[21] Chantis A N, Belashchenko K D, Smith D L, Tsymbal E Y, Schilfgaarde M van and Albers R C 2007 *Phys. Rev. Lett.* **99** 196603
[22] Moser J, Zenger M, Gerl C, Schuh D, Meier R, Chen P, Bayreuther G, Wegscheider W, Weiss D, Lai C H, Huang R T, Kosuth M and Ebert H 2006 *Appl. Phys. Lett.* **89** 162106
[23] Zhang X D, Li B Z, Sun G and Pu F C 1997 *Phys. Rev.* B **56** 5484
[24] Schmidt G, Ferrand D, Molenkamp L W, Filip A T and Wees B J van 2000 *Phys. Rev.* B **62** R4790
[25] Dresselhaus G 1955 *Phys. Rev.* **100** 580
Wang Z G and Zhang P 2007 *Chin. Phys.* **16** 517
[26] Yang M and Li S S 2005 *Phys. Rev.* B **72** 193310
[27] Perel V I, Tarasenko S A, Yassievich I N, Ganichev S D, Belkov V V and Prettl W 2003 *Phys. Rev.* B **67** 201304(R)
[28] Moodera J S, Kinder L R, Wong T M and Meservey R 1995 *Phys. Rev. Lett.* **74** 3273
[29] Meservey R and Tedrow P M 1994 *Phys. Rep.* **238** 173
[30] Moodera J S and Kinder L R 1996 *J. Appl. Phys.* **79** 4724
[31] Groner M D, Elam J W, Fabreguette F H and George S M 2002 *Thin Solid Films* **413** 186
[32] Wu H C, Guo Y, Chen X Y and Gu B L 2003 *J. Appl. Phys.* **93** 5316
[33] Rössler U and Kainz J 2002 *Solid State Commun.* **121** 313
[34] R Winkler 2003 *Springer Tracts in Modern Physics* (Berlin: Springer) p55
[35] Ganichev S D, Bel'kov V V, Golub L E, Ivchenko E L, Schneider P, Giglberger S, Eroms J, De Boeck J, Borghs G, Wegscheider W, Weiss D and Prettl W 2004 *Phys. Rev. Lett.* **92** 256601
[36] Wang L G, Yang W, Chang K and Chan K S 2005 *Phys. Rev.* B **72** 153314
[37] Cheng J L, Wu M W and da Cunha Lima I C 2007 *Phys. Rev.* B **75** 205328